

Experimental Energy and Angular Distributions of Inner Bremsstrahlung

T. B. NOVEY

Chemistry Division, Argonne National Laboratory, Lemont, Illinois

(Received September 29, 1952)

The spectra of the continuous radiation or inner bremsstrahlung emitted in the beta-decay of P^{32} and RaE have been measured in the region of 20–250 kev with a NaI scintillation spectrometer. Comparison of the spectra on an absolute basis with the prediction of the theory shows good agreement.

The angular correlation of the radiation with the emitting beta-particles was also measured. The results are in excellent agreement with theoretical predictions.

I. INTRODUCTION

THE continuous radiation known as inner bremsstrahlung emitted in the process of beta-decay has been studied experimentally over a period of twenty-five years. A series of measurements has been made using ionization chambers or G-M tube detectors where little or no energy resolution was possible. The most recent of these were by Wu¹ and by Stahel and Guillessen² in which the average radiation energy per emitted beta-particle in the decay of P^{32} and RaE was determined with integrating ionization chambers. The integral radiation intensity was found to agree with theory.

The theory of the process was developed independently by Knipp and Uhlenbeck³ and by Bloch⁴ for allowed beta-transitions assuming the polar vector interaction and recently was extended by Wang Chang and Falkoff⁵ and Madansky *et al.*⁶ for forbidden transitions and other interaction types. The cross section for radiative transition per beta-particle was shown to be insensitive to the degree of forbiddenness or type of interaction responsible for the birth of the beta-particle, so no information is needed concerning nuclear wave functions in order to calculate the radiation intensity and angular correlation to a good approximation.

The development in recent years of scintillation detectors and in particular of thallium-activated sodium iodide scintillators has made it possible to make measurements with good energy discrimination and high efficiency on this type of a low probability process involving the emission of low energy gamma-radiation. Measurements of this type have been undertaken independently by Madansky and Rasetti⁷ and the author. Preliminary reports have been published on the measurements reported in this paper.⁸

In this work the inner bremsstrahlung spectra of P^{32} and RaE have been measured experimentally and

compared on an absolute basis with the theory in the range of 20 to 250 kev. The angular correlation between the beta-particles and the radiations has also been measured in the angular range of 30° to 180°, and the shapes have been compared with those predicted theoretically. In both cases agreement with theory is obtained.

II. ENERGY SPECTRA

A. Apparatus

The apparatus used is shown schematically in Fig. 1. The source is evaporated from aqueous solution over an area of 0.3 cm² on a thin plastic film (50 $\mu\text{g}/\text{cm}^2$) which is located at a distance of 20 cm from a NaI(Tl) scintillator 1 $\frac{1}{4}$ in. in diameter and $\frac{1}{2}$ in. thick. A lead collimator is located halfway between the source and detector. Over the collimator is placed a 1.03 g/cm² beryllium absorber, which is thick enough to absorb completely the beta-radiations coming from the source. A rough estimate of the outer bremsstrahlung produced in the beryllium can be obtained by extrapolation of the measurements of Wu,¹ who found experimentally that the ratio of outer bremsstrahlung to inner bremsstrahlung produced when P^{32} radiations are absorbed in aluminum is about four to one, in agreement with theory.

Wu also showed that the total intensity of outer bremsstrahlung produced when electrons are completely absorbed is approximately proportional to the first power of the atomic number of the absorber and not to the square as is the case for single nuclear scattering. This decreased dependency on Z is due to the fact that the number of nuclei encountered by an electron in its range depends inversely upon the atomic number of the absorber.

For the case of absorption in beryllium the amount of outer bremsstrahlung produced is then about 4/13 of that produced in aluminum, and so the ratio of outer to inner bremsstrahlung is close to unity.

As the paths of the electrons in the beryllium are winding, the resultant outer bremsstrahlung distribution would be expected to be nearly isotropic.

The amount of inner bremsstrahlung passing through the collimator hole and into the detector is equal to the amount of outer bremsstrahlung produced in the

¹ C. S. Wu, Phys. Rev. **59**, 481 (1941); references to earlier papers are given here.

² E. Stahel and J. Guillessen, J. phys. et radium **1**, 12 (1940).

³ J. K. Knipp and G. E. Uhlenbeck, Physica **3**, 425 (1936).

⁴ F. Bloch, Phys. Rev. **50**, 272 (1936).

⁵ C. S. Wang Chang and D. L. Falkoff, Phys. Rev. **76**, 365 (1949).

⁶ Madansky, Lipps, Bolgiano, and Berlin, Phys. Rev. **84**, 596 (1951).

⁷ L. Madansky and F. Rasetti, Phys. Rev. **83**, 187 (1951).

⁸ T. B. Novey, Phys. Rev. **84**, 145 (1951); **86**, 619 (1952).

beryllium over the collimator hole. The latter, however, is emitted isotropically, and so only a small portion is detected as given by the geometrical efficiency of the detector for a source at the position of the collimator. This efficiency is 0.6 percent for ten centimeter spacing between collimator and detector, and so the percentage of outer to inner bremsstrahlung reaching the detector is about 0.6 percent.

All other parts of the apparatus are located at a distance of at least 20 cm from the source so that very little of the outer bremsstrahlung which is produced in the eventual absorption of the source radiations can be detected. The space between the collimator and the detector, and the detector itself is completely shielded by two inches of lead in order to prevent detection of scattered photons.

The sodium iodide detector is assembled in a moisture-proof container with a 0.013-inch thick aluminum window and is optically coupled through a short Lucite light pipe to a 5819 photomultiplier tube. The pulses are fed from a cathode follower preamplifier into a linear amplifier and sliding single-channel pulse-height analyzer designed by R. Swank of this laboratory. The spectrometer was calibrated with photon lines of known energies 22, 84, and 667 keV from Cd^{109} , Tm^{170} , and Cs^{137} . The energy resolution widths at half-height were 57 percent, 30 percent, and 11 percent, respectively.

The channel width on the analyzer was selected in the light of the above energy resolutions to be at least a factor of four smaller than the line resolution at any given energy.

B. Source Preparation

The P^{32} sources were prepared by evaporating high specific activity P^{32} solution newly obtained from Oak Ridge National Laboratory. One-millicurie sources were used. The sources were evaporated on $50 \mu\text{g}/\text{cm}^2$ LC-600 films. The active solution was spread over an area of 0.3 cm^2 with the help of dilute insulin solution. The source weight was less than $25 \mu\text{g}$. The films were supported on aluminum rings of outer diameter 2 in., inner diameter $1\frac{1}{2}$ in., and thickness 0.015 in.

The RaE was extracted from a RaDEF mixture on a semimicro scale using a separation based upon the precipitation of RaE (bismuth) with iron hydroxide in dilute sodium hydroxide solution, the RaD (lead) with added lead holdback carrier remaining in solution. The RaD is thoroughly removed by a few reprecipitations as indicated by the elimination of the 47-keV gamma-peak in the spectrum. The iron is ether-extracted, and the RaF plated out onto silver powder in 0.5N HCl until less than 1 percent remains. The RaE was carried on a few micrograms of aluminum hydroxide which was carefully washed, slurried up, transferred to the film, and evaporated to dryness.

Great care was taken to remove all of the lead in the final RaE separations. In the preparation of the source for the measurements described in the preliminary

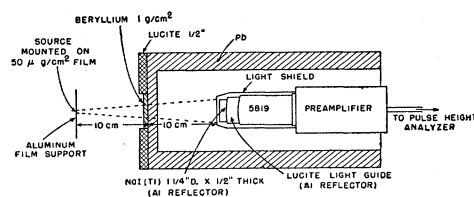


Fig. 1. Arrangement of apparatus for measurement of inner bremsstrahlung spectra.

communication⁸ about twenty micrograms of lead were left in the source. This was sufficient to result in the production of twice as much outer bremsstrahlung as inner in the source and caused the high results reported.

The absence of outer bremsstrahlung production in the final sources was demonstrated by measuring the gamma-spectrum and then spreading the source over a twofold larger area, Fig. 8. As the intensity did not change appreciably, source thickness effects were not affecting the results.

C. Corrections to the Spectra

1. Background

Background was determined at the various energies by placing a $7.5 \text{ g}/\text{cm}^2$ lead absorber over the collimator hole.

2. Resolution

Correction for the finite energy resolution of the scintillation spectrometer was made using the expression given by Palmer and Laslett.⁹ The corrected spectrum N_T is given by

$$N_T(E) = N_e(E) - KN_e'(E) - \frac{1}{2}KEN_e''(E), \quad (1)$$

where

$$K = W^2(E)/(0.693 \cdot 2E).$$

$W(E)$ is the half-width at half-height of a peak produced by photons of energy E . N_e , N_e' , N_e'' are the experimental spectrum and its first and second derivatives, respectively.

3. Absorption

Corrections for absorption of the radiation in $1.03 \text{ g}/\text{cm}^2$ of beryllium (beta-absorber) and $90 \text{ mg}/\text{cm}^2$ of aluminum (NaI container cover) were made using absorption coefficients given by Compton and Allison.¹⁰ A plot of the correction factors A_{Be} and A_{Al} is shown in Fig. 2. The absorption coefficient for the beryllium absorber was checked at 22 and 84 keV using monochromatic gamma-sources in order to make sure the beryllium did not contain any appreciable heavy element impurities. Agreement was obtained to a few percent.

⁹ J. P. Palmer and L. J. Laslett, Atomic Energy Commission Report AECU-1220 (March 14, 1951), unpublished.

¹⁰ A. H. Compton and S. K. Allison, *X-Rays in Theory and Experiment* (D. Van Nostrand Company, Inc., New York, 1935), Appendix IX.

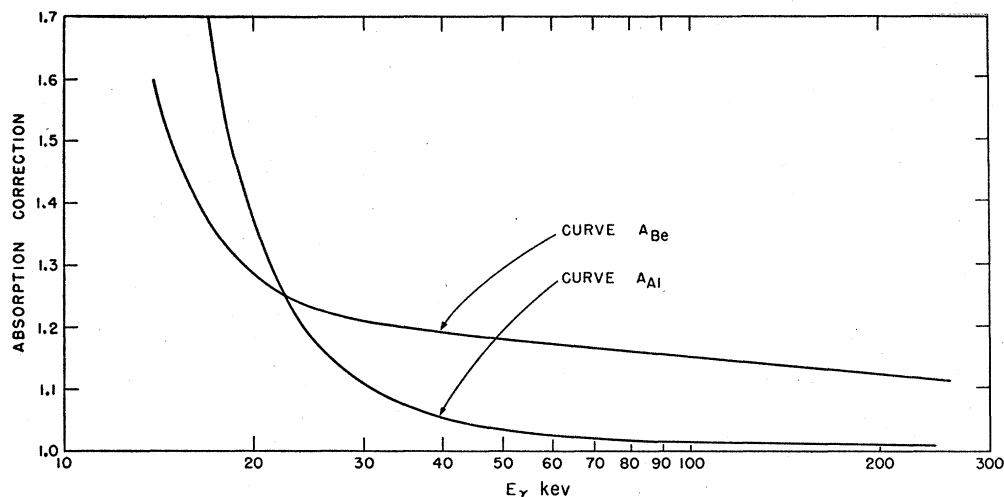


FIG. 2. Absorption factors for photons in 1.03 g/cm^2 Be (curve A_{Be}) and 0.090 mg/cm^2 Al (curve A_{Al}).

Absorption in the 20-cm air path was negligible in the energy range investigated.

4. Gamma-Detection Efficiency

In determining the spectral shape, it is important that all of the photons detected give their full energy to the scintillator as the presence of Compton continua will smear out the curve. For the $\frac{1}{2}$ -inch thick crystal used the former condition holds very well up to 250 keV although at this energy the Compton and photoelectric cross sections are equal. This is due to secondary reaction of the Compton scattered photons which result in the full energy being dissipated in the crystal. This effect is shown in Fig. 3. Curve B shows the fraction of the pulses falling in the photoelectric peak compared to the sum of the areas in the photoelectric peak and the Compton continuum as a function of the incident photon energy based on a series of unpublished measurements by D. Engelkemeir of this laboratory. Curve A shows the fraction of the total cross section that is derived from photoelectric absorption. The efficiency ϵ_γ calculated from the total cross section in NaI is shown in Fig. 4.

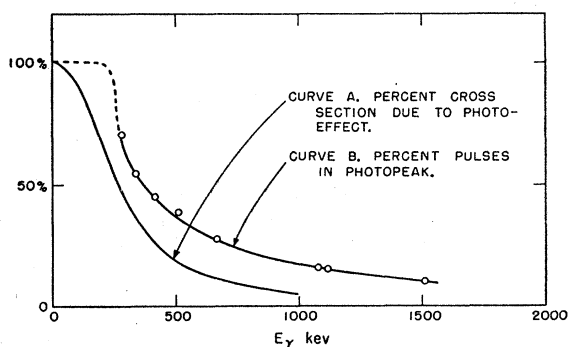


FIG. 3. Comparison of percentage of photoelectric to total absorption cross section (curve A) with percentage of scintillation pulses falling in the photoelectric peak (curve B) for photon absorption in a $\frac{1}{2}$ -inch thick NaI(Tl) crystal.

Thus although the gamma-efficiency is diminishing and the Compton cross section becomes comparable to the photoelectric cross section, in the region up to 250 keV the spectrum measured is almost entirely due to pulses arising from complete absorption of the photons. As the intensity of photons drops off very rapidly with energy, the contribution of the Compton continua from higher energy photons can be neglected in these measurements.

The accuracy of this calculated efficiency decreases in the region of 200–250 keV owing to the onset of edge effects.

5. Iodine K X-Ray Escape

The escape of iodine K x-rays from the detector following photoelectric absorption near the surface becomes important in the region just above the K edge of iodine at 34 keV and results in the shifting of photon pulses down in energy by the K x-ray energy 29 keV.

The magnitude of the escape was calculated on an infinite plane approximation which is satisfactory in the present case of a surface $1\frac{1}{4}$ in. in diameter. The edge effects are small owing to the high absorption coefficient of the iodine K x-rays in sodium iodide ($T_{\frac{1}{2}} = 0.01 \text{ in.}$). The photons are assumed to be normally incident, and the x-rays are emitted isotropically. The probability that a photon will undergo a photoelectric effect and the x-ray escape is then

$$P_e = \frac{\mu_\gamma}{2} \int_0^\infty \int_0^{\pi/2} \exp\{-[\mu_\gamma + (\mu_x/\cos\theta)]x\} \sin\theta d\theta dx, \quad (2)$$

where μ_γ is the incident photon absorption coefficient, μ_x is the iodine K x-ray absorption coefficient, x is the depth of penetration into the surface, and θ is the angle between the directions of the normal to the surface and the emitted x-ray. Upon integration this becomes

$$P_e = 0.5 \left[1 - \frac{\mu_x}{\mu_\gamma} \ln \left(1 + \frac{\mu_\gamma}{\mu_x} \right) \right]. \quad (3)$$

A graph of P_e is shown in Fig. 5 for the escape of iodine K x-rays (28.7 keV). The net correction p to the continuous spectra, taking into account the fact that loss of the x-ray shifts the pulses to lower apparent energy, is shown in Fig. 6.

This net correction was made assuming from the theory (Sec. E) that the probability spectrum varies approximately inversely with energy so that the number of photons per unit energy interval at energy $E_\gamma - 28.7$ keV is equal to $E_\gamma - 28.7/E_\gamma$ of the number at energy E_γ . If the loss of pulses at energy E_γ due to K x-ray escape is p_1 and that at $E_\gamma - 28.7$ keV is p_2 , then the net fractional loss p at $E_\gamma - 28.7$ keV is $p_2 - p_1(E_\gamma - 28.7/E_\gamma)$. The net correction changes sign abruptly at the K edge because at this point p_2 suddenly becomes zero. A smoothed-out correction was used because the resolution correction could not completely reconstruct the sharp K edge effect.

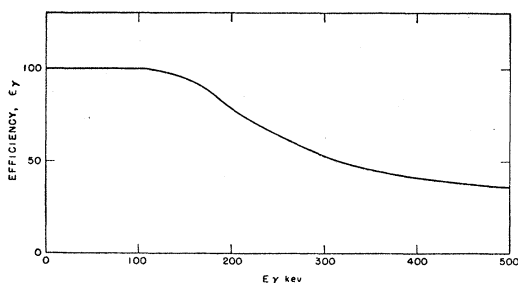


FIG. 4. Gamma-efficiency of 1/2 inch thick NaI crystal calculated from total absorption cross section for normally incident photons.

6. Geometrical Efficiency

The geometry factor was calculated using the formula

$$G = a^2/4r^2 = 0.16 \text{ percent}, \quad (3)$$

where a , the crystal radius, is 1.6 cm and r , the distance to the edge of the crystal face, is 20 cm.

7. Source Calibration

The source disintegration rates R were determined by reference to lower activity sources which were calibrated using a 4π proportional counter and standard RaDEF¹¹ sources. The ratios of activities of the high and low activity sources were determined by counting on an end window flow type proportional counter through an absorber selected to bring the activities into the counting rate range of the counter.

8. Normalization

The spectra were normalized to unit mc^2 energy interval by dividing the data by the analyzer window width Δk in units of mc^2 , converted to energy intensity by multiplication by the energy k in units of mc^2 , and normalized to radiation per beta-decay.

¹¹ T. B. Novey, Rev. Sci. Instr. 21, 280 (1950).

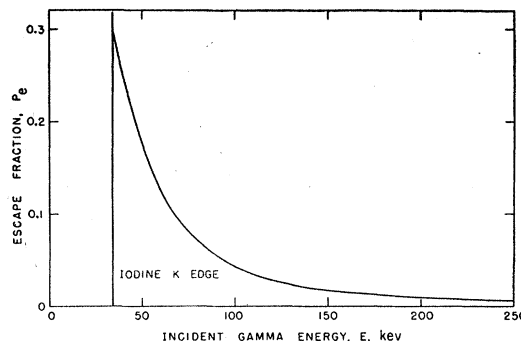


FIG. 5. Calculated fraction of iodine K x-rays escaping from a NaI crystal for normally incident photons.

D. Results

The final result of these corrections is the intensity spectrum $kS(k)$, the radiation intensity per unit energy interval per beta-decay,

$$kS(k) = A_{Be} A_{A1} k N_T / [\epsilon_\gamma (1 - p) GR \Delta k]. \quad (4)$$

The results of two experiments on P³² are shown in Fig. 7. Run 2 was made with the apparatus as described in part A of this section. Run 1 was an earlier run made with somewhat less favorable geometrical conditions. The source to detector distance was 15 cm, the absorber was Lucite instead of beryllium, and the collimator opening was 1 1/4 in. in diameter. The estimated outer bremsstrahlung contribution was 5 percent as compared to 0.6 percent for Run 2.

Figure 8 shows the results for RaE for the source as originally prepared and the source spread over a twofold larger area. In the latter case it was necessary to use the larger 1 1/4 inch collimator.

E. Comparison with Theory

It has been shown by Wang Chang and Falkoff⁵ that, in the low energy photon region in which most of the

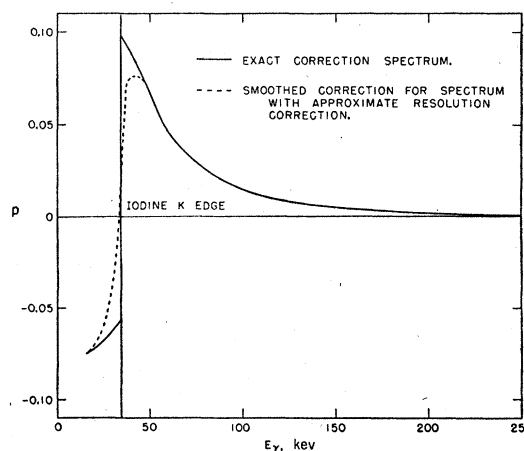


FIG. 6. Net correction to the spectrum resulting from escape of K x-rays.

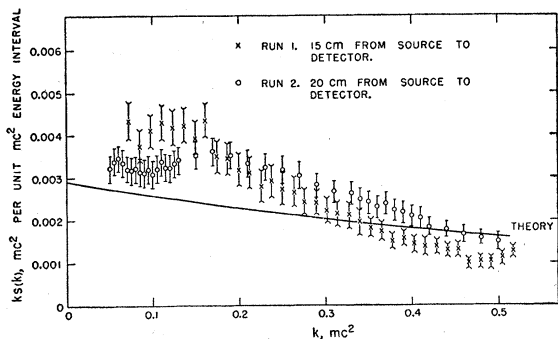


FIG. 7. P^{32} inner bremsstrahlung spectrum, $kS(k)$, mc^2 per unit mc^2 energy interval vs k in units of mc^2 .

radiation occurs and in which these studies were made, the intensity per beta-particle is insensitive to the degree of forbiddenness or the nature of the interaction involved in the beta-decay process and that, to an accuracy well within limits set by these measurements, the emission probability $S(k)$ can be factored as follows:

$$S(k) = \int_{1+k}^{W_0} P(W_e) \Phi(W_e, k) dW_e, \quad (5)$$

where $P(W_e)$ is the normalized beta-spectrum for which the experimental spectrum may be used and

$$\Phi(W_e, k) = \frac{\alpha p_s}{\pi p_e k} \left\{ \frac{(W_e^2 + W_s^2)}{W_e p_s} \ln(W_s + p_s) - 2 \right\}, \quad (6)$$

where W_e is the "created" electron energy; p_e is the "created" electron momentum, $(W_e^2 - 1)^{1/2}$; W_s is the observed electron energy, $(W_e - k)$; p_s is the observed electron momentum, $[(W_e - k)^2 - 1]^{1/2}$; α is the fine structure constant, $1/137$; and k is the photon energy. All energies are in units of mc^2 , and all momenta in units of mc .

This factoring implies that the beta-decay and radiation can be considered to be independent processes.

Equation (5) was integrated numerically using normalized energy spectra obtained from P^{32} and RaE spectra given respectively by Siegbahn¹² and Neary.¹³ The results multiplied by the photon energy k in order to remove the low energy divergence are shown as the solid lines in Figs. 7 and 8.

These theories neglect the effect of nuclear charge on the radiation, but it has been shown by Hellund (unpublished calculations) that these effects are unimportant.

Both the P^{32} and RaE spectra show a peaking in the region of 80 keV. One would expect an amount of K x-rays from RaE due to electronic excitation during beta-decay of the order of $0.6/Z^2$ or 10^{-4} K x-ray per beta-decay.¹⁴ This is in rough agreement with the

¹² K. Siegbahn, Phys. Rev. **70**, 133 (1946).

¹³ G. J. Neary, Proc. Roy. Soc. (London) **A175**, 71 (1940).

¹⁴ A. Migdal, J. Phys. (U.S.S.R.) **IV**, 449 (1941).

number of photons corresponding to the area in the peak in the RaE curve. In addition to this, some K x-rays arising from photoelectric absorption of outer or inner bremsstrahlung in the faces of the conical slit would contribute to both curves.

The higher intensity shown in P^{32} , Run 1, at low energies is probably due to the larger amount of outer bremsstrahlung present in this case. The effect would tend to concentrate at low energies because the multiple scattering process involved in beta-absorption would lower the average energy of the radiating electrons and thus lower the average energy of the bremsstrahlung.

In view of the above considerations and the difficulties involved in the accurate application of the many correction factors described in Sec. II C, these measurements are considered to be in good agreement with the predictions of the theory.

III. BETA-INNER BREMSSTRAHLUNG ANGULAR CORRELATION

A. Experimental

The apparatus is shown schematically in Fig. 9. A plastic vacuum chamber is used to reduce electron scattering and outer bremsstrahlung production. The chamber body is made of $\frac{1}{8}$ -inch Bakelite-impregnated fiber tubing and the top and bottom of $\frac{1}{2}$ -inch Bakelite using O rings for vacuum seals. The sources are mounted on thin films supported on an aluminum ring in turn supported by a Lucite mount centered in the chamber.

The electron detector is a stilbene crystal cemented into a Lucite light guide which is in turn cemented onto the face of a 5819 photomultiplier tube with Gelva V-1.5 cement. A unit of this type can be assembled in an oven at 75°C after careful warming of the crystal wrapped in several layers of cleansing tissue. The Gelva cement should previously have been melted in a vacuum and dissolved gases pumped out.

The face of the crystal is coated with a very thin layer of silicone stopcock grease and 0.2 mg/cm^2 aluminum foil adhered to the surface to serve as a light reflector and to reduce the rate of sublimation in the vacuum.

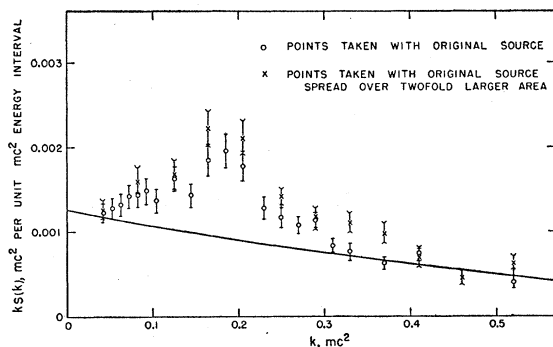


FIG. 8. RaE inner bremsstrahlung energy intensity spectrum, $kS(k)$, mc^2 per unit mc^2 energy interval vs k in units of mc^2 .

The vacuum seal is made by means of an O ring seal to the tube face.

The chamber and detector are fastened to a table which can be automatically rotated in 15° steps at predetermined time intervals. The timing clock also trips a single-frame movie camera which records the necessary counting data from the scaling circuit registers.

The gamma-detector is a NaI(Tl) scintillator as described in Sec. II. The pulses are double delay line shaped¹⁵ to reduce the pulse width below 0.1 μsec. A diagram of the coincidence system is shown in Fig. 10. The pulses are fed through distributed line amplifiers with a gain of 100 on each side, delay line shaped, and fed through cascades to a 12AT7 coincidence mixer and to trigger pairs delivering 0.3-μsec pulses. The output of the mixer drives a trigger pair delivering a 0.5-μsec pulse. The trigger-pair pulses are fed into a simple crystal diode triple coincidence circuit to insure that only pulses which have been recorded as singles counts can record as a coincidence.

The coincidence circuit was designed and built by B. Norris of this laboratory and was designed to be used in conjunction with the 200-ohm distributed line amplifiers which are available commercially. The coincidence circuit has built into it pulse shaping delay lines which allow pulses to be shaped at 0.015, 0.03, 0.075, and 0.15 microsecond width. The minimum resolving time of the coincidence circuit is thus 0.03 microsecond. For this experiment the stilbene pulses were shaped at 0.015 μsec. In conjunction with the double delay line pulse shaping of the sodium iodide pulses at 0.075 μsec, the measured resolving time was about 0.11 microsecond. Owing to the fact that the pulse size of the photon pulses is reduced by a factor of about 7 by the pulse shaping networks, for low energy photons the pulse sizes begin to fall into the tube noise region. Consequently, in order to obtain a high detection efficiency, i.e., close to 100 percent for photons of energies down to 40 keV, it is necessary to operate at a photomultiplier voltage such that the noise background is of the order of a few thousand counts per minute. The beta-particles are detected down to energies of about 50 keV. Thus the coincidences detected are

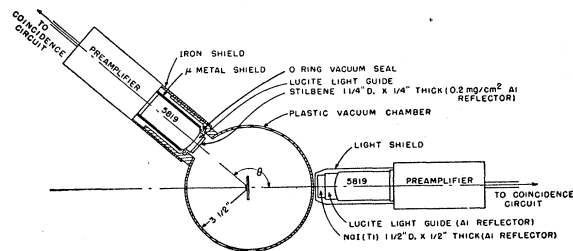


Fig. 9. Beta-gamma angular correlation apparatus.

¹⁵ T. B. Novey and D. W. Engelkemeir, Rev. Sci. Instr. 22, 841 (1951).

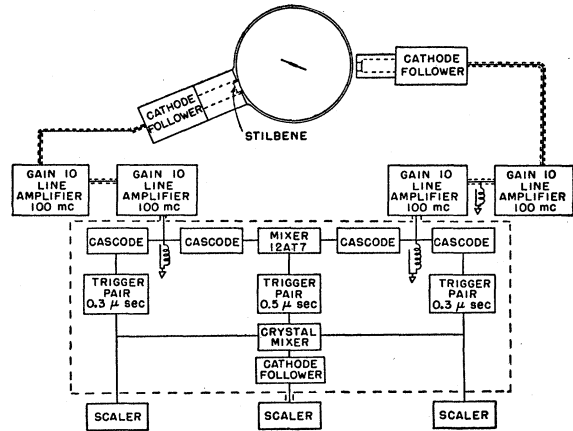


Fig. 10. Block diagram of electronic circuitry for beta-inner bremsstrahlung angular correlation measurements.

between β-particles of energies down to 50 keV and photons with energies down to about 40 keV.

The experimental angular correlation measurements were made at angles from 180° to 45° on both sides. In the case of P³² a point at 33° was obtained by crowding the detectors as close as possible. The correlation curves thus obtained were averaged and corrected for the finite angular resolution (20° full detector angle, about 1 percent geometrical efficiency).

The chance contributions to the coincidence rates were measured carefully as they were often equal to or greater than the true rates. The measurement was made using duplicate sources located and shielded so that while the singles rates and the pulse-height distributions were the same as with the single source, no true coincidences could occur.

As will be shown in the next section, no inner bremsstrahlung radiation is emitted in the directions colinear with the electron path, i.e., at 0° and 180°. Thus, the chance rate should equal the total coincidence rate at 180°. This agreement was never obtained probably owing to some contribution from scattering in the apparatus.

The rates at 180° varied from 10 to 15 percent above the measured chance rates, and the excesses amounted to 10 to 15 percent of the true rates at 35°. When the source and detectors were suspended in air with as much material as possible removed from around them to a distance of one or two feet, these percentages decreased to 5 percent.

It was not known whether this "scattering" correction was constant with angle between the detectors, but as it was small compared to the true coincidence rate at low angles, it was added to the chance rate and subtracted as a constant from the total coincidence rate. The correlation curves could not be compared to the theory on an absolute basis as the efficiency of the coincidence circuit is not well known but were normalized to agree at 45°.

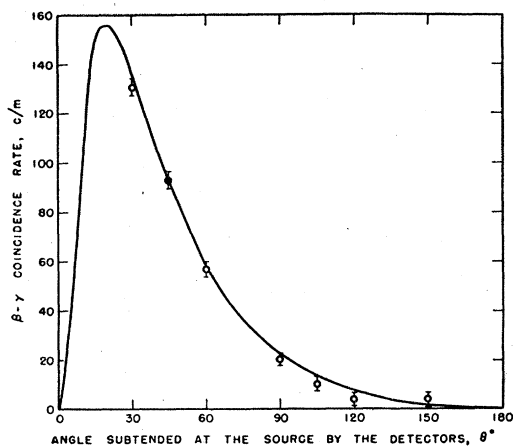


Fig. 11. Beta-inner bremsstrahlung angular correlation in P^{32} . Comparison of experiment (circles) with theory (solid line) normalized at 45° , Φ .

The data are given by the points in Figs. 11 and 12.

B. Comparison with Theory

The approximations valid for $k \ll W_{e \max}$ which were used in Sec. II E in obtaining the inner bremsstrahlung spectra also hold for the experimental conditions of the angular correlation measurements, and as shown by Wang Chang and Falkoff⁵ and Madansky *et al.*,⁶ the correlations for low energy photons are insensitive to the degree of forbiddenness or type of interaction involved in the beta-decay. To be sure, if the correlation of higher energy photons were measured, as pointed out by the latter authors, there would be a considerable effect. As the number of these photons is very low, the measurement is difficult, though not impossible with high efficiency liquid scintillators and very fast ($2\tau \sim 10^{-9}$ sec) coincidence circuits.

The probability $d\Phi$ that a beta-particle emitted with energy W_e will radiate a photon of energy k per unit photon energy interval at an angle θ between \mathbf{k} and \mathbf{p}_e is given by

$$d\Phi(W_e, k, \theta) = \frac{\alpha p_s}{4\pi^2 p_e k} \left[\frac{W_e^2 + W_s^2}{W_e(W_s - p_s \cos\theta)} - \frac{1}{(W_s - p_s \cos\theta)^2} - 1 \right] d\Omega_k. \quad (7)$$

As shown by Wang Chang and Falkoff⁵ on the assumption that k is small and thus that $W_e = W_s$, $P_e = P_s$ and as $P/W = \beta$, $W^2 = 1/1 - \beta^2$, Eq. (7) becomes

$$d\Phi = \frac{\alpha}{2\pi k} \frac{\beta^2 \sin^3\theta}{(1 - \beta \cos\theta)^2} d\theta,$$

or

$$\frac{d\Phi}{d\Omega}(W, k, \theta) = \frac{\alpha}{4\pi^2 k} \frac{\beta^2 \sin^3\theta}{(1 - \beta \cos\theta)^2}. \quad (8)$$

They also obtained this result by a purely classical relativistic calculation.

For the case at hand this must be integrated over the beta-spectrum detected and the range of gamma-energies detected; thus,

$$\frac{d\Phi(\theta)}{d\Omega} = \frac{\alpha}{4\pi^2} \int_{W_{\min}}^{W_{\max}} \int_{k_{\min}}^W \frac{P(W)\beta^2 \sin^3\theta}{k(1 - \beta \cos\theta)^2} dk dW, \quad (9)$$

where k_{\min} is the detector energy cutoff at 40 keV. The minimum beta-energy detected is about 50 keV, and as electrons below this energy produce essentially no radiation above 40 keV, the beta lower limit can be

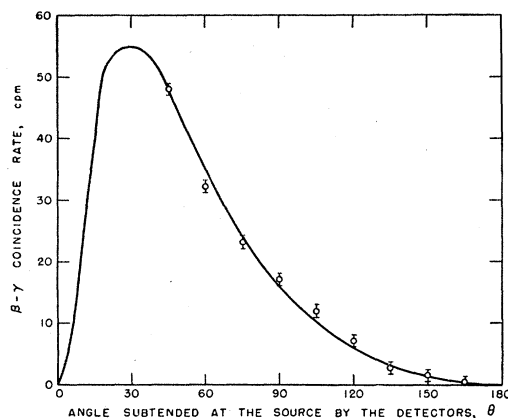


Fig. 12. Beta-inner bremsstrahlung angular correlation in RaE. Comparison of experiment (circles) with theory (solid lines) normalized at 45° .

taken as zero. Integrating over the photon energy Eq. (8) becomes

$$\frac{d\Phi(\theta)}{d\Omega} = \frac{\alpha}{4\pi^2} \int_0^{W_{\max}} \ln(W/k_{\min}) \times P(W) \frac{\beta^2 \sin^3\theta}{(1 - \beta \cos\theta)^2} dW. \quad (10)$$

This expression was evaluated numerically, and the normalized results are shown as the solid lines in Figs. 10 and 11.

The experimental angular correlation is an excellent agreement with that predicted by the theory.

I wish to express my appreciation to Dr. E. Hellund who gave much time to theoretical investigation of problems arising during this research, and to Dr. D. Engelkemeir for many helpful discussions during the course of the experiments and for permission to include some of his unpublished data in this paper.